MARS CLIMATE DATABASE v1.0

CRITICAL REVIEW

(ESTEC Contract 11369/95/NL/JG)

M. Collins and S.R. Lewis

June 5, 1997

Contents

1 Introduction

The Mars Climate Database (MCD) is a database of atmospheric statistics compiled from state-of-the art Global Circulation Model simulations of the Martian atmosphere. The models used to compile the statistics have been extensively validated using available observational data and represent the current best knowledge of the state of the Martian atmosphere given the observations and the physical laws that govern the atmospheric circulation and surface conditions on the planet.

This document compares the MCD with such observational data as is available concerning the atmosphere of Mars and with previous martian atmospheric models which have been developed for similar purposes, such as MarsGRAM (Justus, 1990). More detailed descriptions of the models used to compile the MCD and of the validation procedures are available in other documents and publications relating to this project (Collins and Lewis, 1997a, 1997b; Collins *et al.*, 1996; Hourdin *et al.*, 1996; Read *et al.*, 1996, 1997).

Note: This document refers to the first release of the Mars Climate Database (MCDv1.0). Future releases will contain updates to the database, to the access software and to the documentation. If you have any queries, or if you want to find out if this is the latest version of the MCD please email `euromars@lmd.ens.fr`.

2 Comparison with Observations

Such observational evidence from the Martian atmosphere as is available and relevant is briefly reviewed in this section and compared where possible with the data contained in the Martian Climate Database and with results from the General Circulation Models which were used in its compilation.

2.1 Dust Distribution

The major factor which governs the inter-annual variability in the martian atmosphere is the amount and distribution of suspended dust. The MCD was compiled with four dust scenarios, two multi-annual simulations for years with constant low dust amounts or moderate dust loading as observed by the Viking landers, and two different seasonal global dust storm scenarios (dust optical depth, $\tau = 2$ and $\tau = 5$). There does indeed appear to be evidence that some martian years are colder (and by implication less dusty), such as the Mariner 9 year and some more recent observations, and some are warmer (and imply more dust in the atmosphere), such as the Viking year (see Figure 1). This is confirmed by the differences in thermal structure between the models run with each dust scenario, see Figure 5 where the low dust run produces an atmosphere with lower temperatures in the regions near the surface perhaps more in accordance with the IRIS observations from Mariner 9. There is good evidence (Zurek *et al.*, 1992) that the dust optical depth may exceed $\tau = 2$ during dust storms and reach $\tau = 5$ or greater; hence the presence of these scenarios in the database. Unfortunately, there are no atmospheric temperature soundings to compare with the model

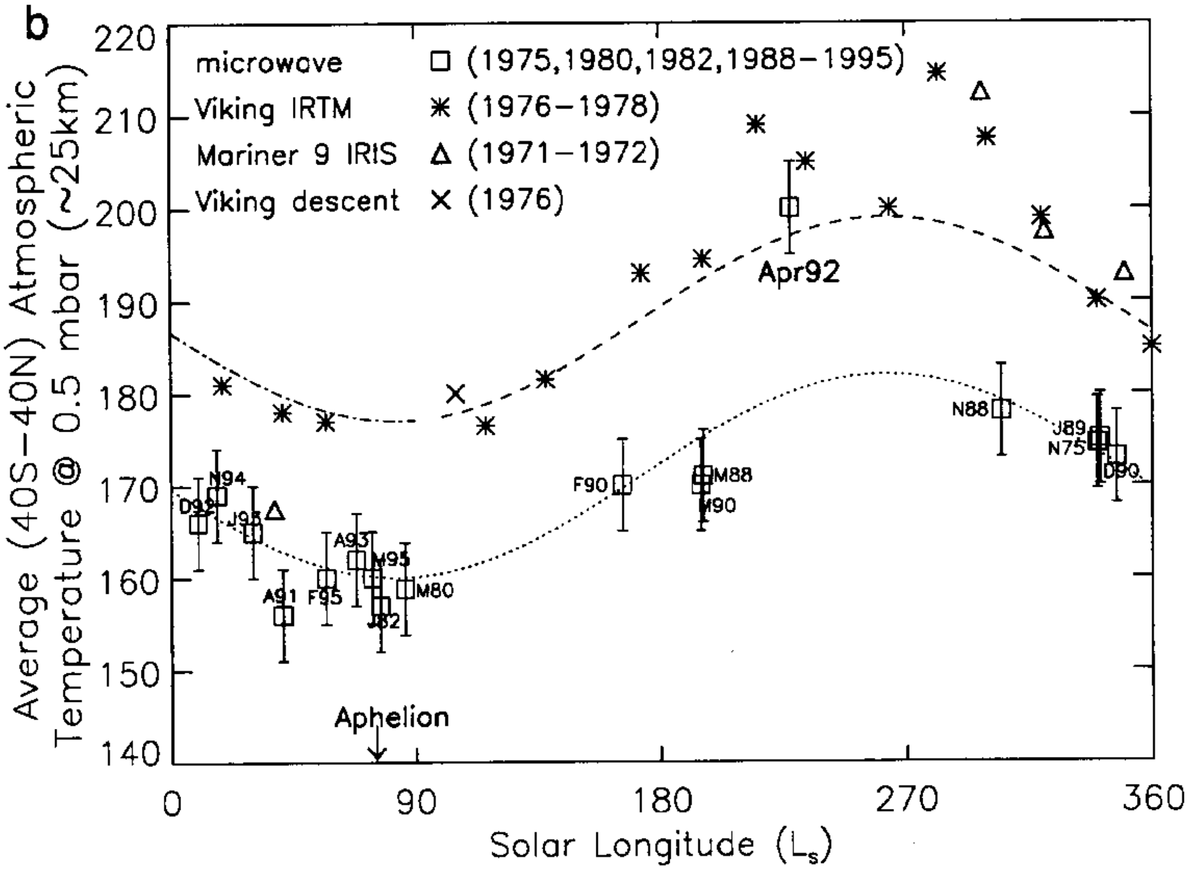

Figure 1: Average (40°S – 40°N) martian atmospheric temperatures at $50\,Pa$ as a function of time of year for observations made in different martian years, including the Viking (1976–1978) and Mariner 9 (1971–1972) periods (from Clancy *et al.*, 1996). The Viking year appears to be significantly warmer than other years, suggesting that the atmosphere contained more dust at that time.

during these periods owing to the difficulties of conducting retrievals in the presence of large dust amounts.

Some of the information from the "Mars Climate Database v1.0: Detailed Design Document" is repeated here for reference. Details of the vertical distribution of the dust in the model are described in the accompanying Detailed Design Document (Collins and Lewis, 1997b).

Baseline multi-annual model integrations were carried out for the database under two main scenarios: (a) seasonally-varying dust as observed during the Viking Lander years, but with the large dust storms removed; and (b) low uniform dust, perhaps appropriate to more recent observations of a clearer, colder Mars. In addition, scenarios were conducted for several seasons with much higher dust loadings, appropriate to dust storm conditions. The details of the scenarios included in the database follow.

- `vik` The standard Viking scenario with data provided for all twelve seasons from multi annual experiments. The total dust optical depth for the Viking case varied as a function of time to fit the Viking observations with peaks representing dust storms removed,

$$\tau(L_S) = 0.7 + 0.3\cos(L_S + 80^\circ) \tag{1}$$

where τ is the optical depth and L_S the solar longitude of Mars. The optical depth was uniform in the horizontal for the Viking baseline run. However, the cut-off of the dust in the vertical varied as a function of both time and latitude,

$$z_{\max}(L_s, \phi) = \left(60 + 18\sin(L_s - 158^\circ) - 22\sin^2\phi\right)\ km \tag{2}$$

where ϕ is the latitude. $z_{\max}$ varies between $78\,km$ at the equator during the dusty seasons and $20\,km$ at the pole during the clear seasons.

- `low` The low dust scenario with data provided for all twelve seasons from multi annual experiments. The low dust case was conducted with a dust distribution which was invariant in latitude, longitude and time, with an optical depth of $\tau = 0.1$ and a cut-off at $z_{\max} = 30\ km$ altitude.
- `ds2` A dust storm with optical depth 2. Data from these runs is only provided for the seasons when dust storms are most likely to occur; seasons 8, 9 and 10. In fact the scenario was initialized from a Viking scenario restart state at the beginning of season 7 and the season 7 data was then discarded. The dust optical depth was set to a constant value of $\tau = 2$, and the vertical cut-off for the dust was modelled as in the Viking scenario, equation 2.
- `ds5` A dust storm with optical depth 5. Data from these runs is only provided for the seasons when dust storms are most likely to occur; seasons 8, 9 and 10. In fact the scenario was initialized from a Viking scenario restart state at the beginning of season 7 and the season 7 data was then discarded. The dust optical depth was set to a constant value of $\tau = 5$, and the vertical cut-off for the dust was modelled as in the Viking scenario, equation 2.

2.2 Surface Pressure

During the Viking mission two landers took meteorological observations for several martian years from the northern hemisphere of the planet (Viking lander 1 was situated at 22° N 48° W and Viking lander 2 was situated at 48° N 226° W). Figure 2 shows the Viking 1 and 2 daily averaged surface pressure observations taken from the first year of the mission. The large seasonal cycle is due to mainly to the condensation and sublimation of CO_2 while the high frequency oscillations are due to weather systems passing over the landers. Figure 3 shows the MCD daily averaged pressure from the Viking sites. The black squares are the 12 seasonal mean pressures and the smooth line is a cubic spline fit to these values. The seasonal cycle in pressure compares well and is due to the fact that there has been an optimisation of polar cap parameters to obtain a best fit (Hourdin *et al.*, 1993). Also shown (as the error bars) is an estimate of the variance due to weather systems simulated in the GCMs. The variance is large in the winter season in good agreement with the observations.

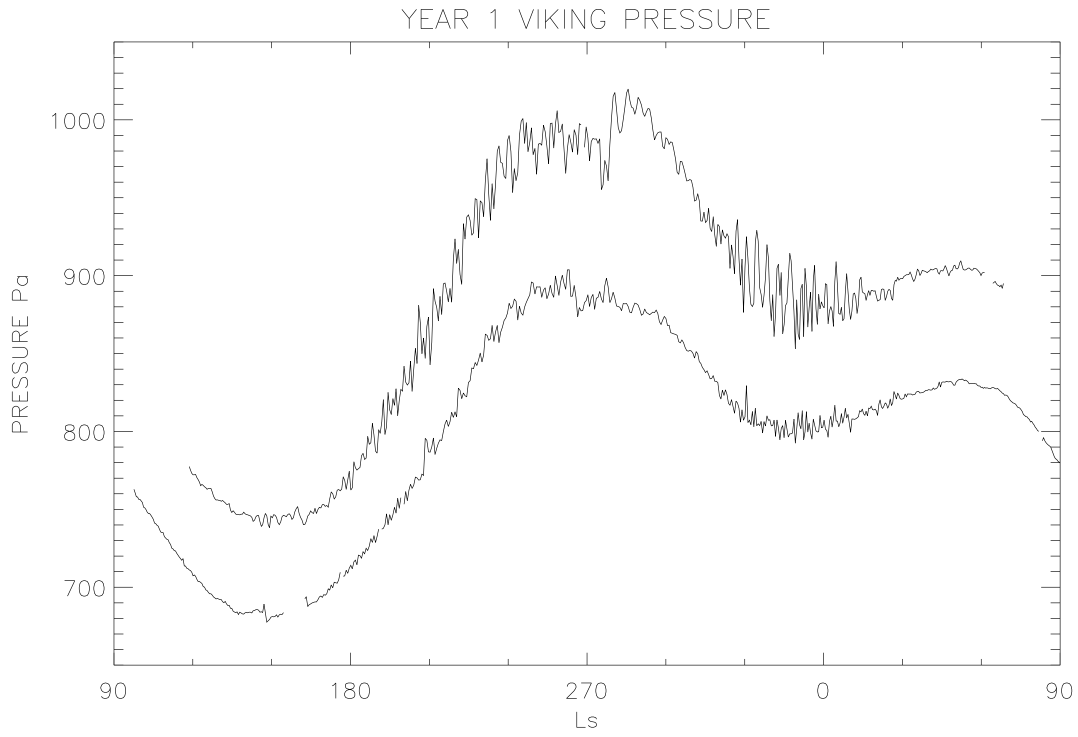

Figure 2: Observed Viking 1 (lower curve) and 2 (upper curve) surface pressure for the first martian year of observations. The high frequency oscillations are due to weather systems passing over the landers.

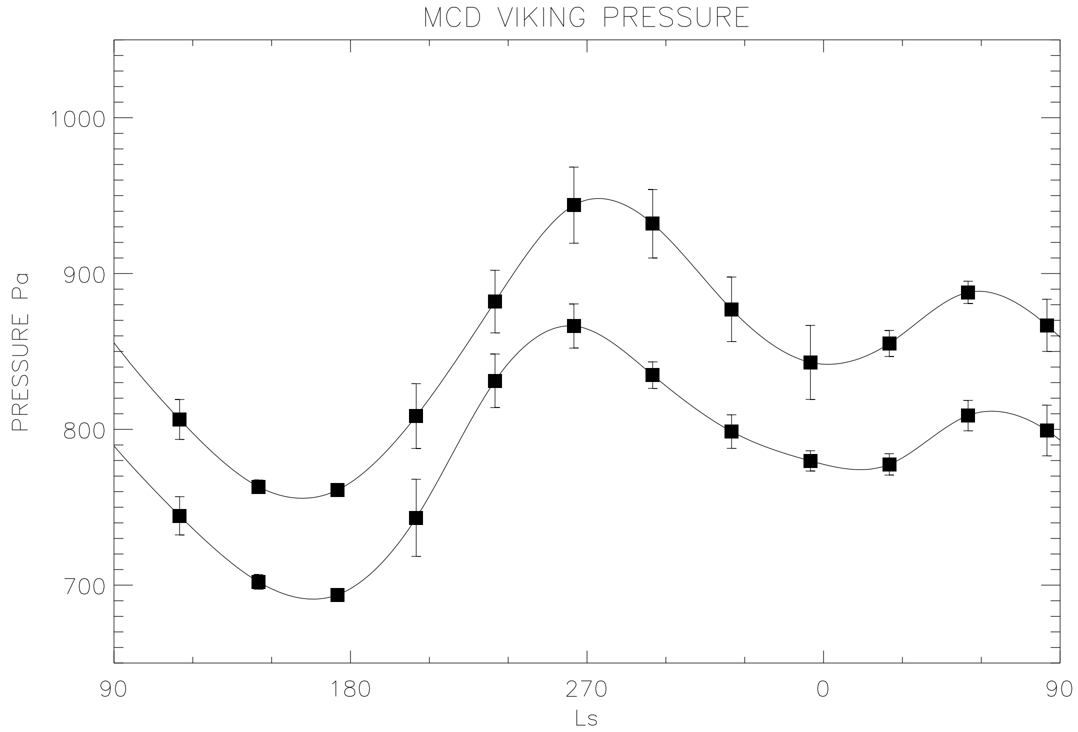

Figure 3: MDC Viking 1 (lower curve) and 2 (upper curve) surface pressure for one martian year. The black squares show the MCD diurnally averaged seasonal values and intervals of $30° L_s$ and the smooth curve is a cubic spline fit to these values. The error bars indicate twice the standard deviation of pressure that is due to weather systems passing over the landers.

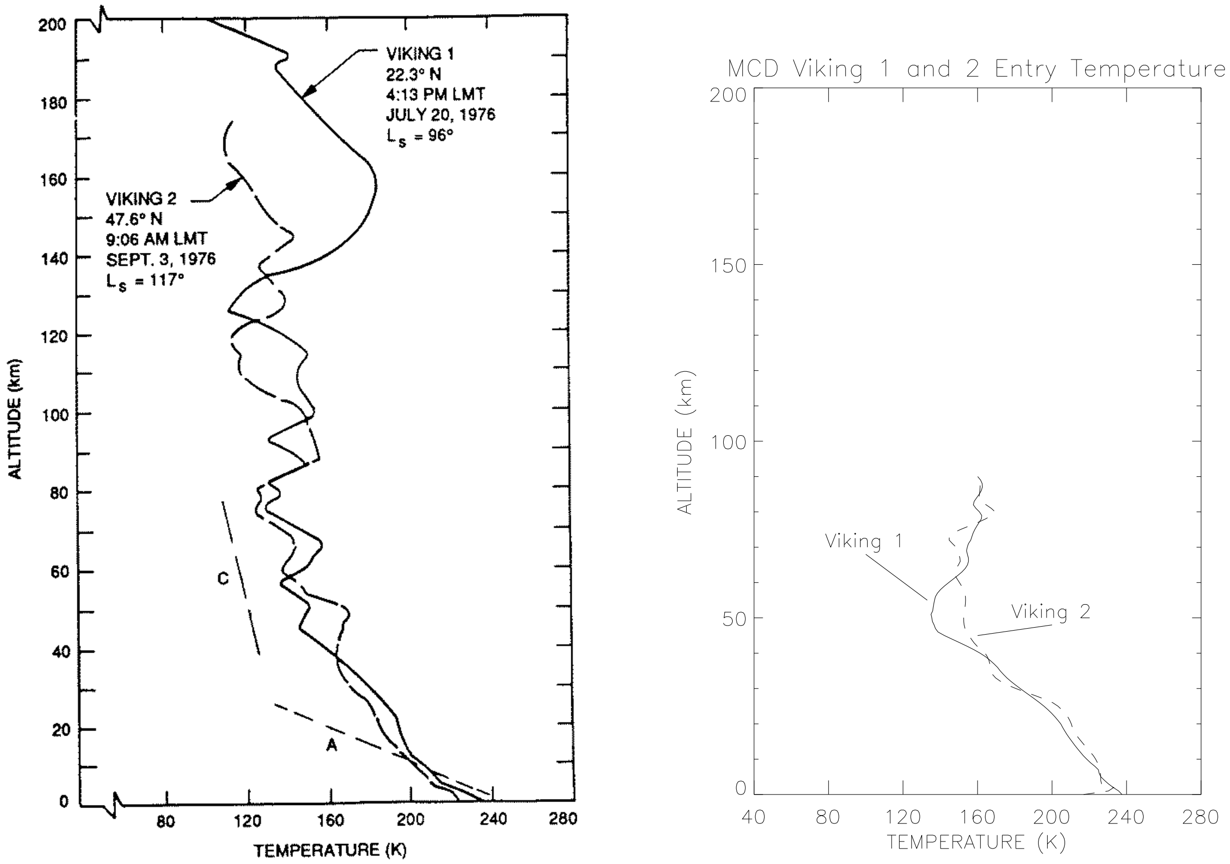

Figure 4: Left: Viking 1 (solid) and Viking 2 (dashed) entry temperature profiles. Right: MCD Viking 1 (solid) and Viking 2 (dashed) entry temperature profiles.

2.3 Temperature

There is various data on temperature from the martian atmosphere from both *in situ* sources and from remote sensing from the Earth and from orbiting spacecraft.

Figure 4 shows temperature measurements taken during the entry phases of the Viking landers. This should be compared with the MCD realisations of these profiles also shown in figure 4. These profiles include a seasonal mean component and a component due to small scale variability representative of vertically propagating gravity waves.

Although the MCD only has data from the surface to approximately 90km the agreement with the observations is good. Using the variability models the user of the MCD can generate many profiles like these.

The majority of temperature observations of the martian atmosphere come from remote sensing of the atmosphere by instruments aboard orbiting spacecraft. Figure 5 shows a comparison of the MCD low and Viking dust scenario mean temperatures with the temperatures derived by Leovy (1982) from the Mariner 9 IRIS instrument. Note in particular the low temperatures at upper levels in the low dust scenario. This is in good agreement with the IRIS temperatures in this region which are colder due to less dusty compared with the spring observed by Viking (Clancy *et al.*, 1996).

Santee and Crisp (1993) also retrieved temperatures from the IRIS instrument from an earlier part of the mission when the atmosphere was dustier. A comparison of their retrievals and the MCD temperatures from the Viking scenario at 2am and 2pm local time are shown in figures 6 and 7. Although it is known that the dust distribution during the Santee and Crisp period is different from that prescribed in the Viking Scenario, there is a broad agreement between the temperatures at both times of day. It can also be noted that the observed temperature structure in the 2pm case is statically unstable (which can be thought to be unrealistic), a feature which the MCD could not predict as any unstable profiles are automatically adjusted to neutral stability in the numerical model.

2.4 Wind

Direct observations of winds on Mars are extremely rare (Zurek *et al.*, 1992). However, winds have been inferred from a variety of secondary effects, such as streak features on the martian surface (Magalhaes, 1987). These observations suffer from the problems of incomplete global coverage and uncertainties in the understanding of exactly how and when the features were formed. Figure 8 shows some wind directions inferred from wind streak data; these can be compared with low level winds from the MCD, shown in Figure 9. Although there are considerable uncertainties in the appropriate dust loading, range of times to average over and heights to sample the winds at, Figures 8 and 9 do show some similarities. In particular, both zonally-averaged diagrams show evidence of predominant westerlies at high northern latitudes, a region of north-easterlies north of the equator with rotation back to westerlies in the southern midlatitudes. There are also similarities in the wind and streak directions in the longitude–latitude maps in several regions where there are observations. The difficulties in interpretation of the streak data make a strict comparison impossible, but the database winds seem plausible at least.

2.5 Polar Caps

Figure 10 shows the time-mean equivalent latitudes for the edges of the polar caps of carbon dioxide ice for the four scenarios from the Martian Climate Database. The equivalent latitude is that which would be reached by a perfectly symmetrical cap occupying the same area as the total area of ice coverage in that hemisphere. Also shown are actual observations of the edges of the martian ice caps, kindly provided by J.B. Pollack (*priv. com.*), for comparison. The agreement appears reasonable.

(a) Temperature (K) observed by Mariner 9 IRIS (L_s = 43°– 54°)

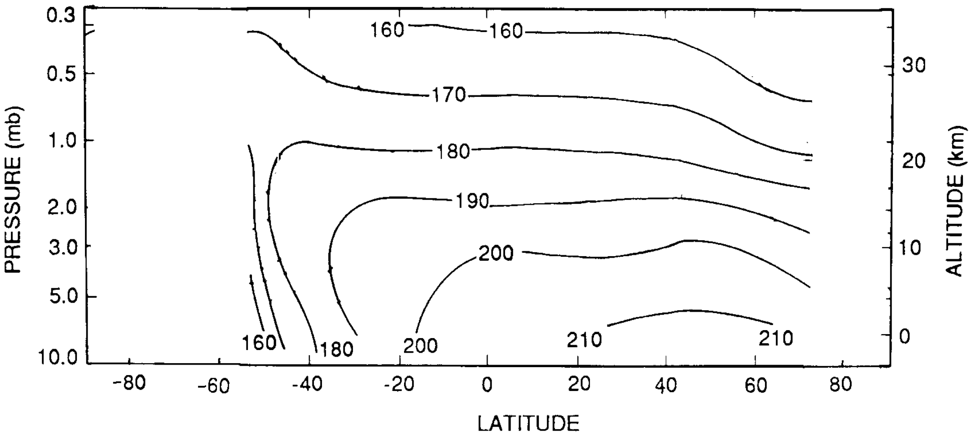

(b) Temperature (K) from the MCD low dust scenario

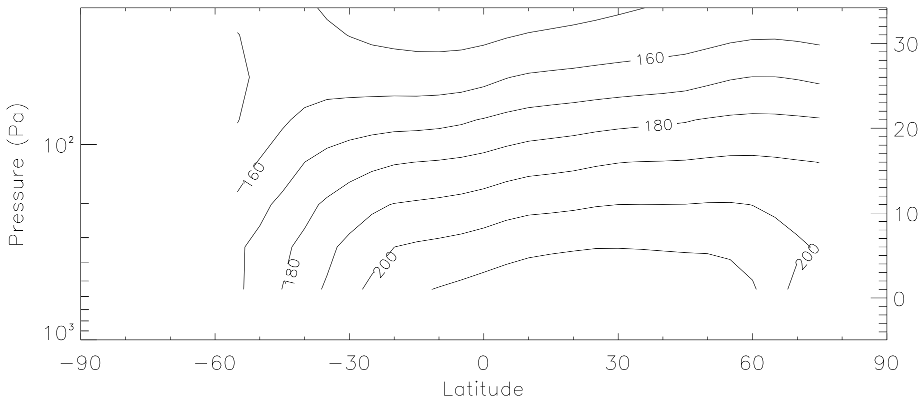

(c) Temperature (K) from the MCD Viking dust scenario

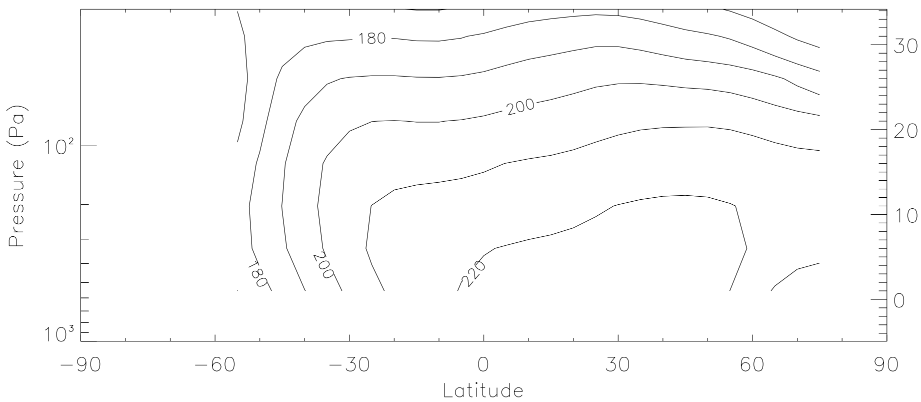

Figure 5: The thermal structure observed by the IRIS instrument on board Mariner 9 in 1972 (from Leovy, 1982) during northern spring (L_s = 43°– 54°), compared to the zonally averaged temperatures from the MCD for the same period for the low and Viking dust scenarios. The spring observed by Mariner 9 is known to have been clearer (and colder) than the spring observed by Viking (Clancy *et al.*, 1996). This is reflected here.

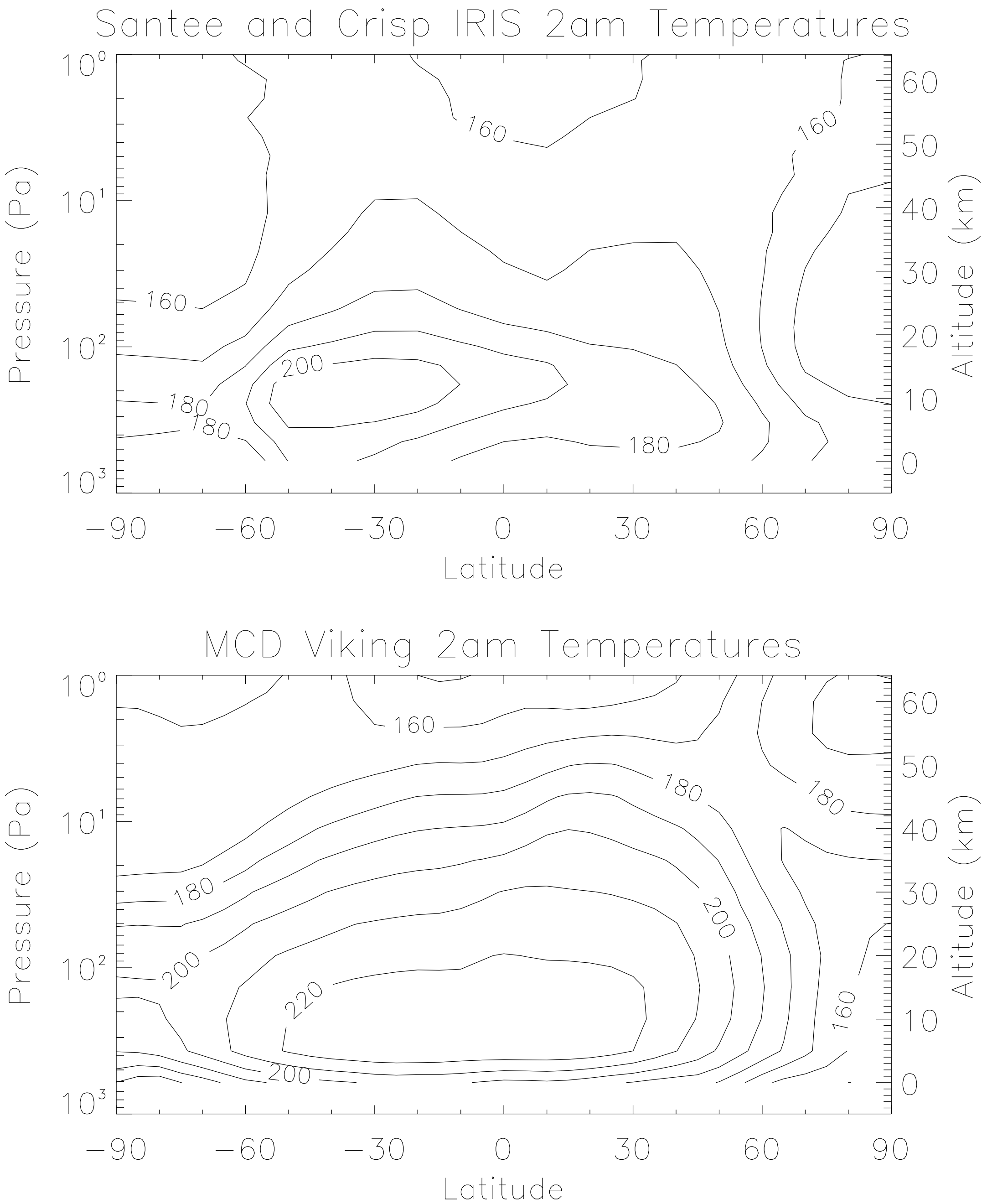

Figure 6: 2 am temperatures for $L_s = 343°$ to $L_s = 348°$ derived by Santee and Crisp (1993) from the Mariner 9 IRIS instrument (upper figure), and the MCD 2am temperatures for this season (lower figure) from the Viking dust scenario.

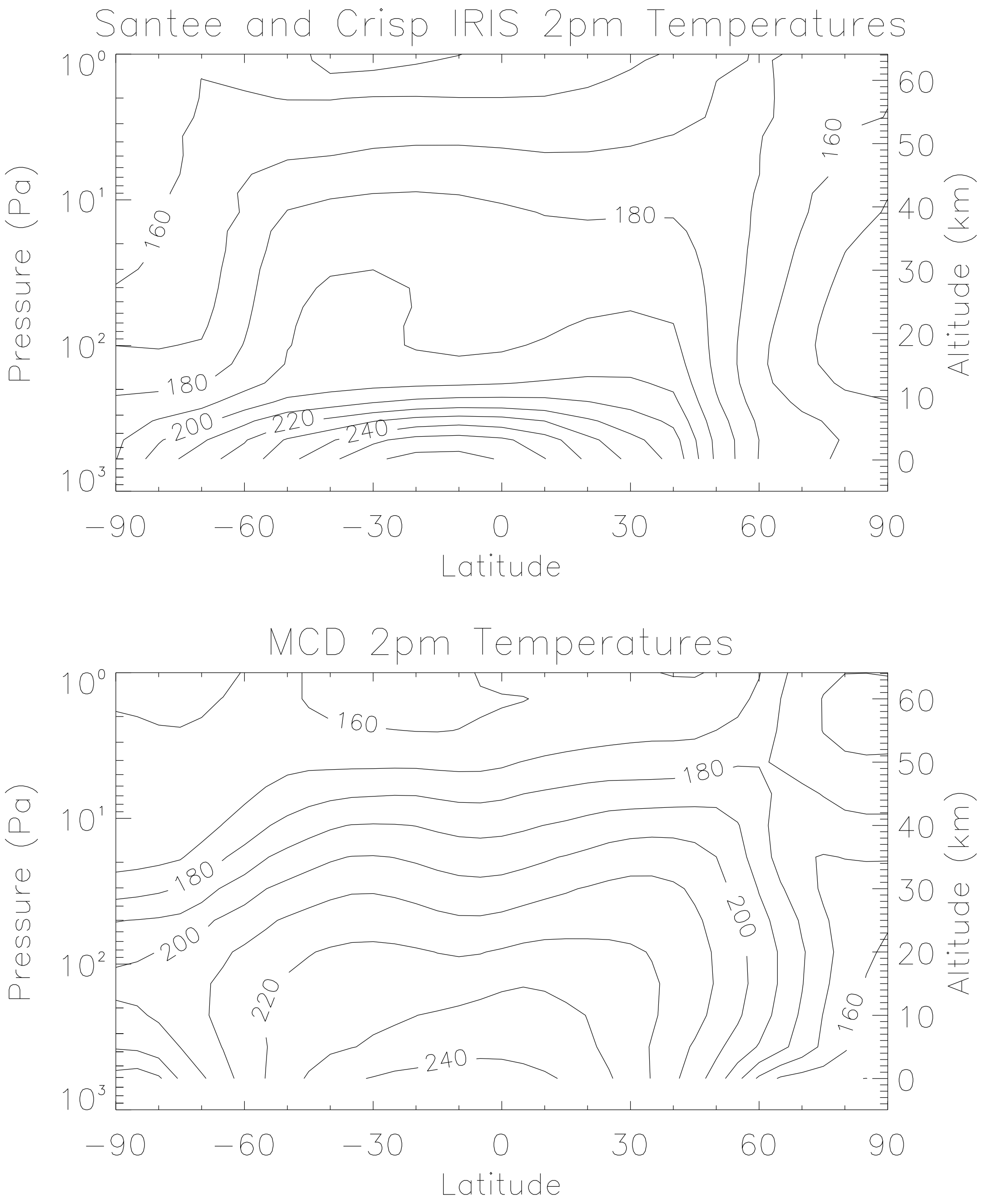

Figure 7: 2 pm temperatures for $L_s = 343°$ to $L_s = 348°$ derived by Santee and Crisp (1993) from the Mariner 9 IRIS instrument (upper figure), and the MCD 2pm temperatures for this season (lower figure) from the Viking dust scenario.

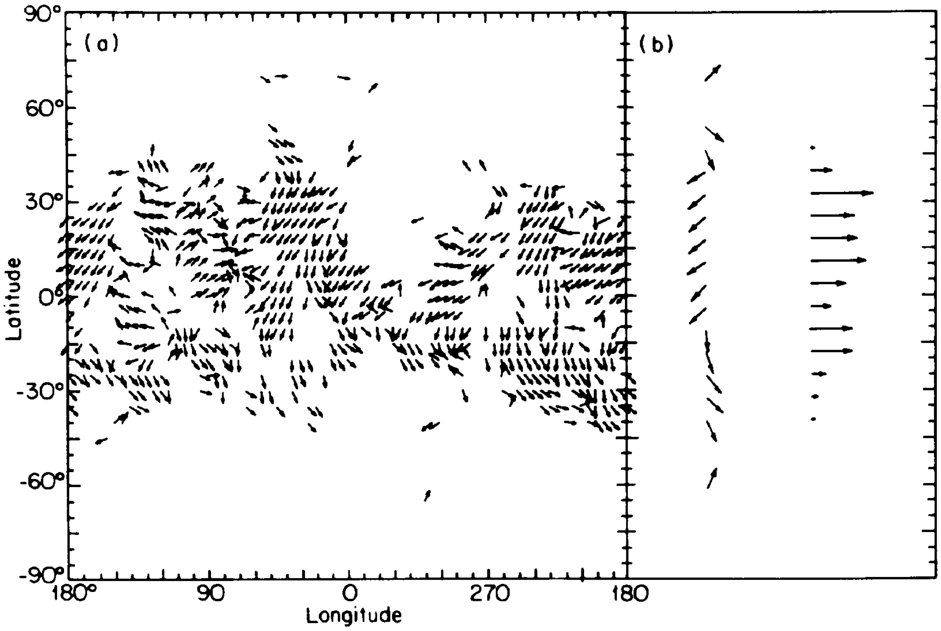

Figure 8: Distribution of "Type I(b)" surface streak orientations derived from Viking Orbiter mosaics (from Magalhaes, 1987): (a) average azimuths for $5° \times 5°$bins; (b) zonally averaged azimuths in $2°$bins (every fourth bin shown), with horizontal arrows representing the relative number of streaks in each bin, the longest of which represents 700 streaks. The "Type I(b)" streaks are thought to indicate the directions of near-surface winds during the decay of the global dust storms in 1977.

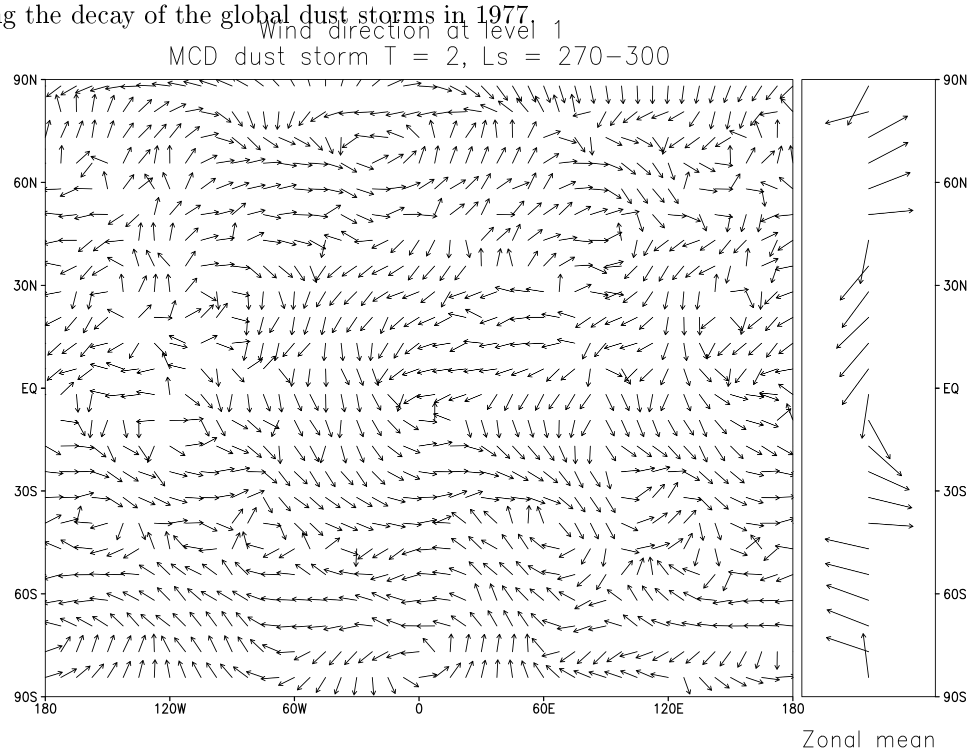

Figure 9: Wind directions taken from the lowest level of the MCD and diurnally-averaged over season 10 ($L_s = 270° - 300°$) of the $\tau = 2$ dust storm scenario. Only every second point in each direction is shown for clarity.

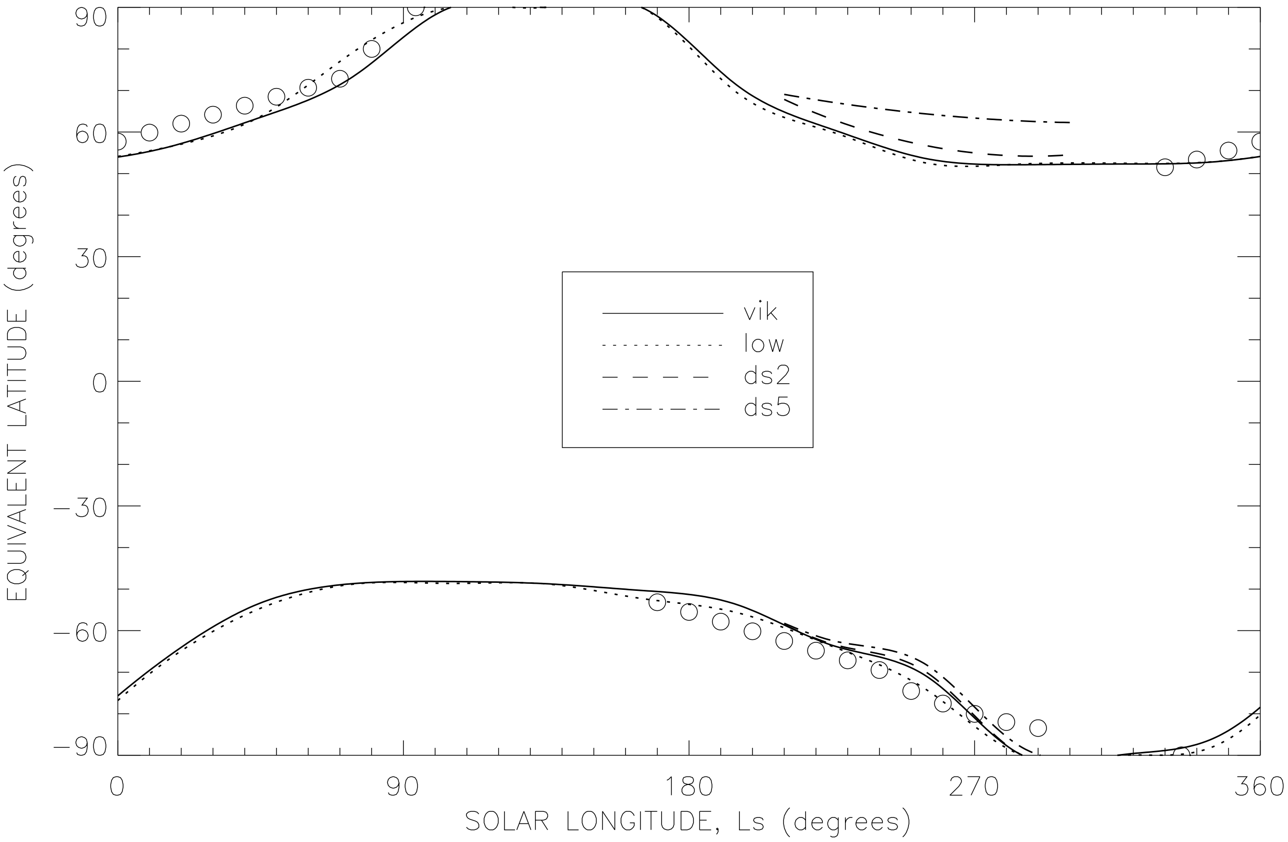

Figure 10: Mean equivalent latitudes for the edges of the polar caps of carbon dioxide ice for the four scenarios from the Martian Climate Database, labelled according to the usual convention. The circles indicate actual observations of the edges of the martian caps, kindly provided by J.B. Pollack (*priv. com.*).

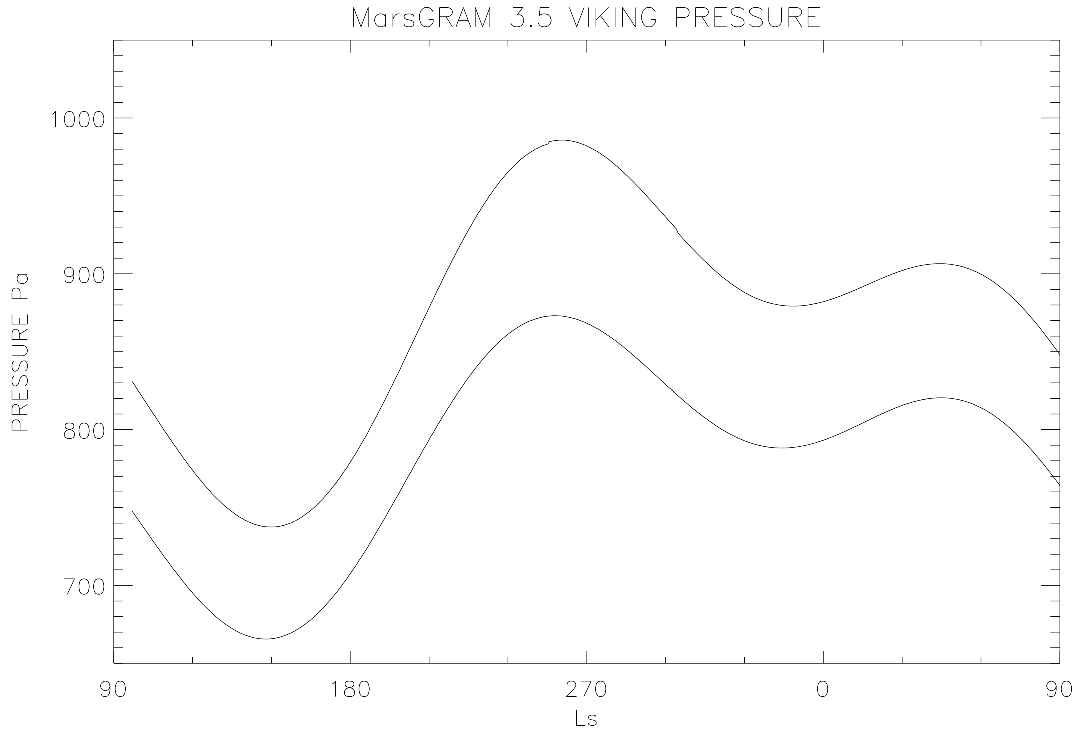

Figure 11: MarsGRAM Viking 1 (lower curve) and 2 (upper curve) surface pressure for one martian year.

3 Comparison with MarsGRAM v3.5

In this section we compare MarsGRAM version 3.5 with the observations and with the MCD.

3.1 Surface Pressure

Figure 11 shows the MarsGRAM v3.5 surface pressure from the Viking lander locations for one year. The agreement with the observed pressure (fig. 2) is very good as MarsGRAM fits a functional form to the observed seasonal pressure. However MarsGRAM provides no information on the synoptic variability whereas the MCD does (the error bars on fig. 3 indicate the amplitude of the synoptic variability). Also it must be noted that not all the seasonal cycle in pressure is due to the condensation-sublimation cycle. Under certain circumstances there can be a significant component due to density gradients within the atmosphere (the dynamical component). This phenomenon shows up when looking at seasonal pressure curves from other points on the planet. Figure 12 shows the daily averaged pressure taken from the Hellas basin (longitude 300° west, latitude 40° south) from the MCD and 13 shows the pressure taken from MarsGRAM. There is a marked difference in the seasonal pressure cycle compared to the pressure cycles at the Viking sites due to the dynamical component. This is one of the key advantages of using the MCD rather than just fitting seasonal pressure curves from the observed Viking data.

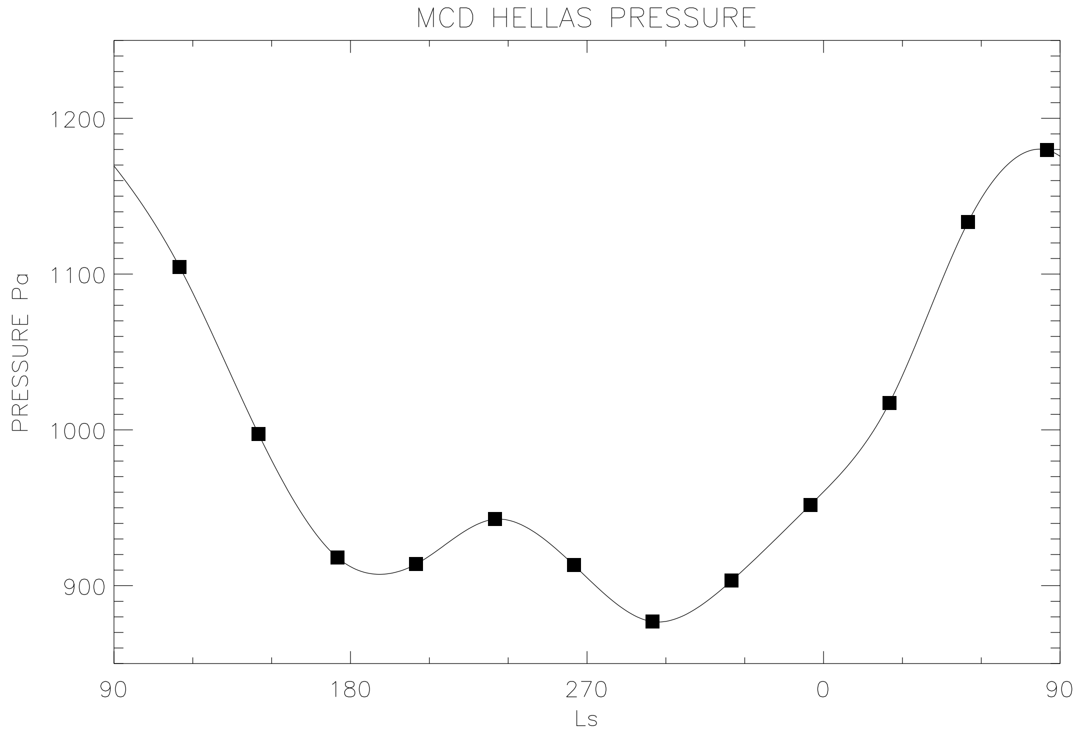

Figure 12: MDC surface pressure for one martian year at longitude 300° west, latitude 40° south, i.e. the Hellas basin. The black squares show the MCD diurnally averaged seasonal values and intervals of $30° L_s$ and the smooth curve is a cubic spline fit to these values.

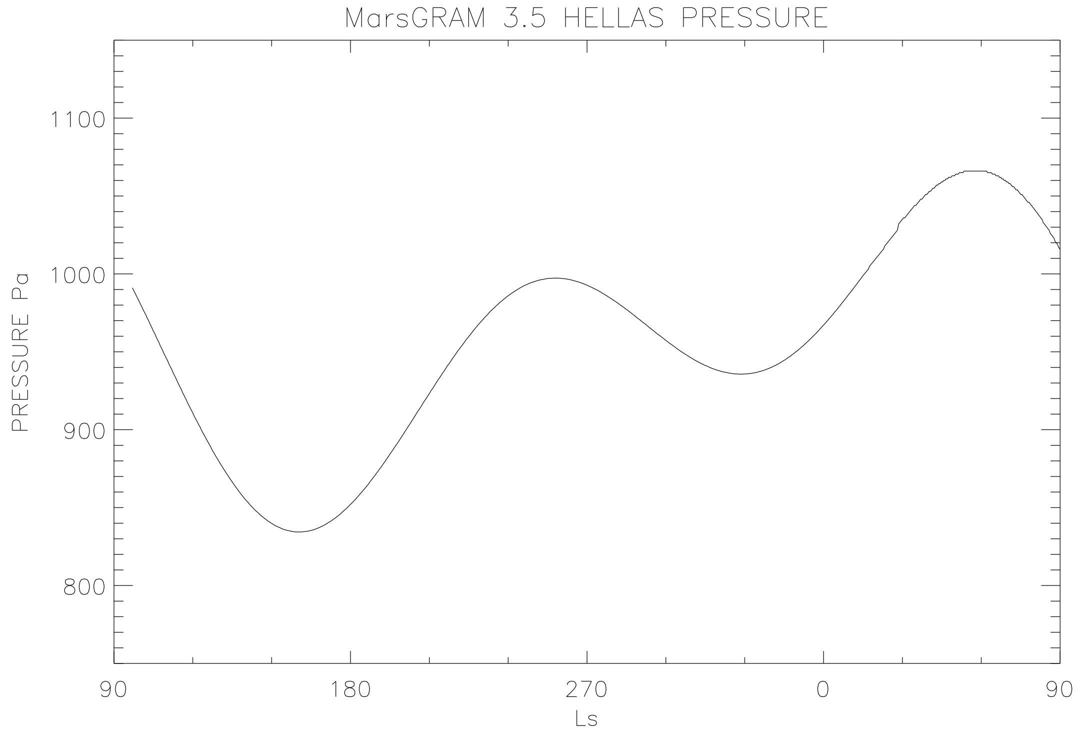

Figure 13: MarsGRAM surface pressure for one martian year at longitude 300° west, latitude 40° south, i.e. the Hellas basin.

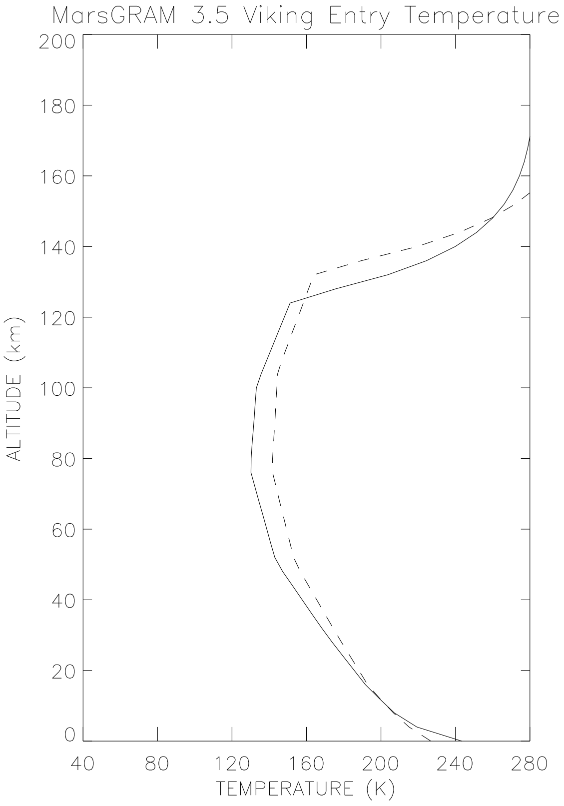

Figure 14: MarsGRAM Viking 1 (solid) and Viking 2 (dashed) entry temperature profiles.

3.2 Temperature

Figure 14 shows the MarsGRAM v3.5 simulated Viking entry temperature profiles to be compared with the observations and the MCD profiles shown in figure 4. Again, MarsGRAM has a good agreement with the mean profile but has no representation of variability. One of the key advantages of MarsGRAM in this case is that it extents upwards of 90km where the MCD has no information, however the agreement with observations is not particularly good in these regions.

The comparison of MarsGRAM v3.5 and the Mariner 9 IRIS temperatures from Leovy (1982) is shown in figure 15. The comparison is very good, especially at upper levels where MarsGRAM captures the cold temperatures at this less dusty season. The agreement is less good towards the north polar regions where MarsGRAM predicts a strong horizontal gradient in temperature. The same can be said of the comparison of MarsGRAM with the Santee and Crisp (1993) temperatures (figs. 16 and 17. However, this good agreement may be due to the fact that in MarsGRAM temperatures a derived using a fit to these observations. The MCD has not been optimised in such a way (the dust distributions, which to a large extent fixes the vertical temperature gradient, have been chosen to represent a wide range of possible conditions on Mars, not the specific observational conditions) so the fit could only be good to a first approximation. Also, as pointed out above, the 2pm observed temperatures are statically unstable and therefore maybe unphysical as unstable profiles would trigger convection in the atmosphere that would make the temperature profile neutral.

(a) Temperature (K) observed by Mariner 9 IRIS ($L_s = 43°– 54°$)

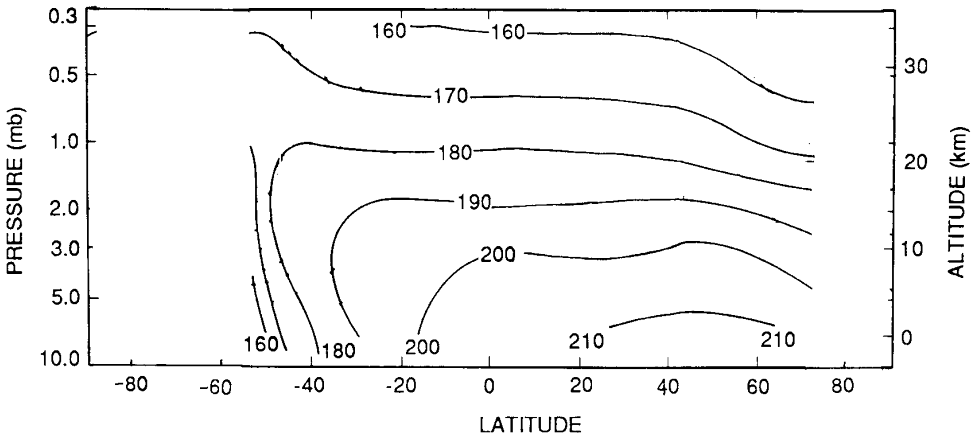

(b) Temperature (K) from MarsGRAM

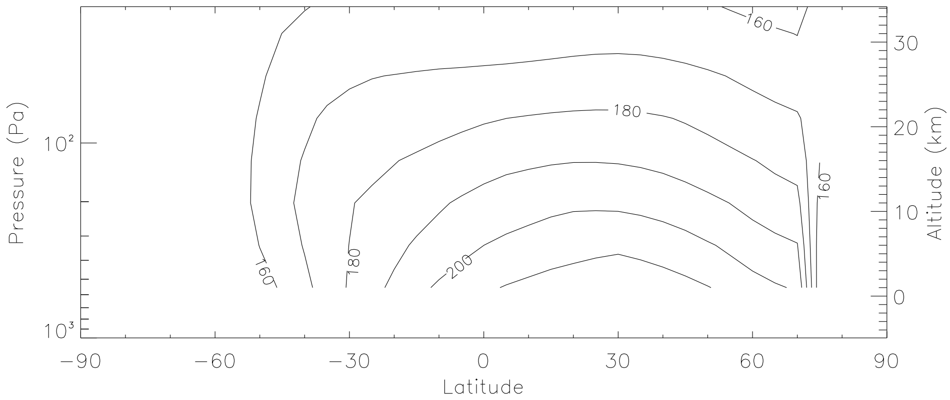

Figure 15: The thermal structure observed by the IRIS instrument on board Mariner 9 in 1972 (from Leovy, 1982) during northern spring ($L_s = 43°– 54°$), compared to the zonally averaged temperatures from MarsGRAM.

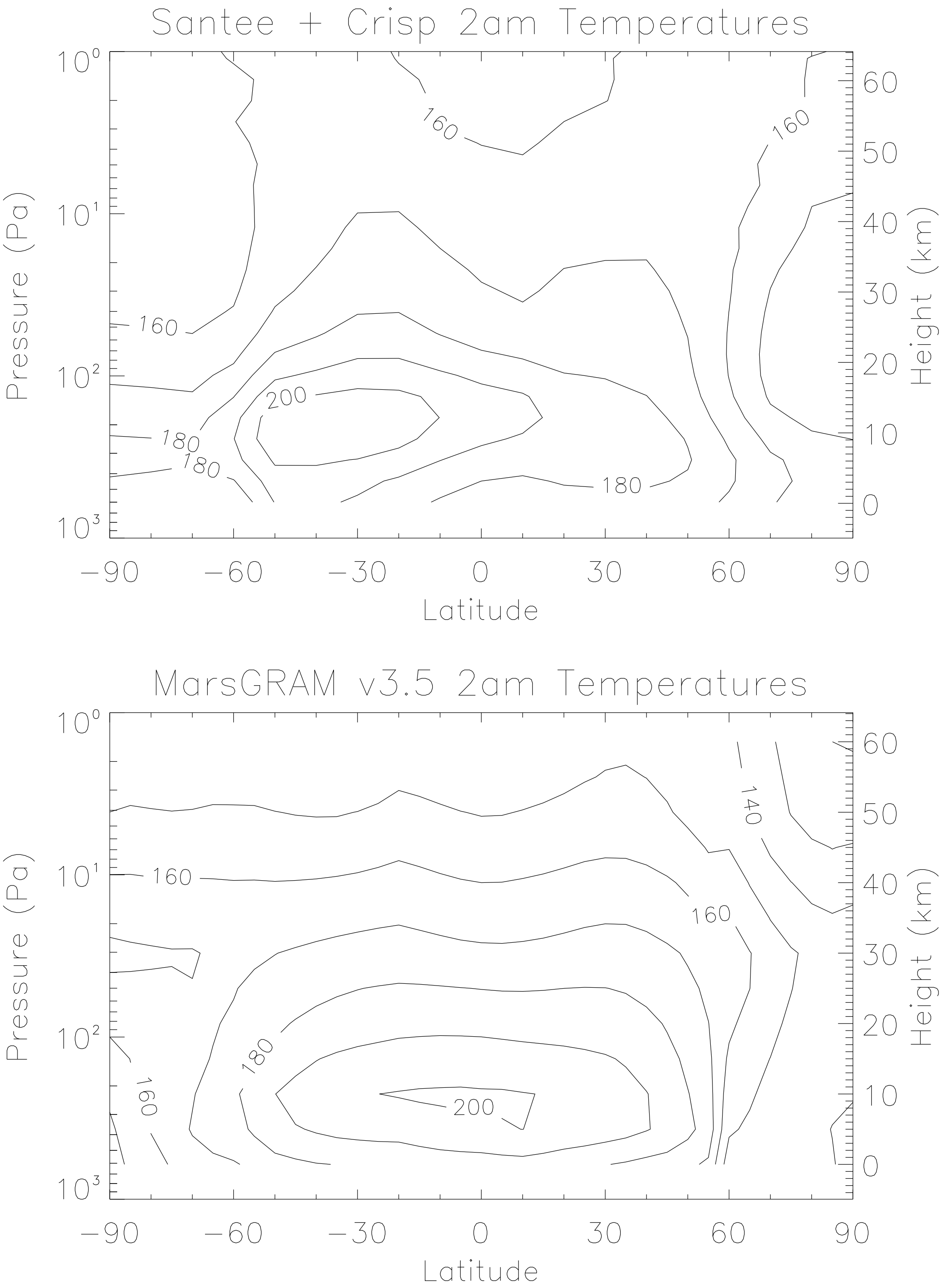

Figure 16: 2 am temperatures for $L_s = 343°$ to $L_s = 348°$ derived by Santee and Crisp (1993) from the Mariner 9 IRIS instrument (upper figure), and the MarsGRAM 2am temperatures for this season (lower figure).

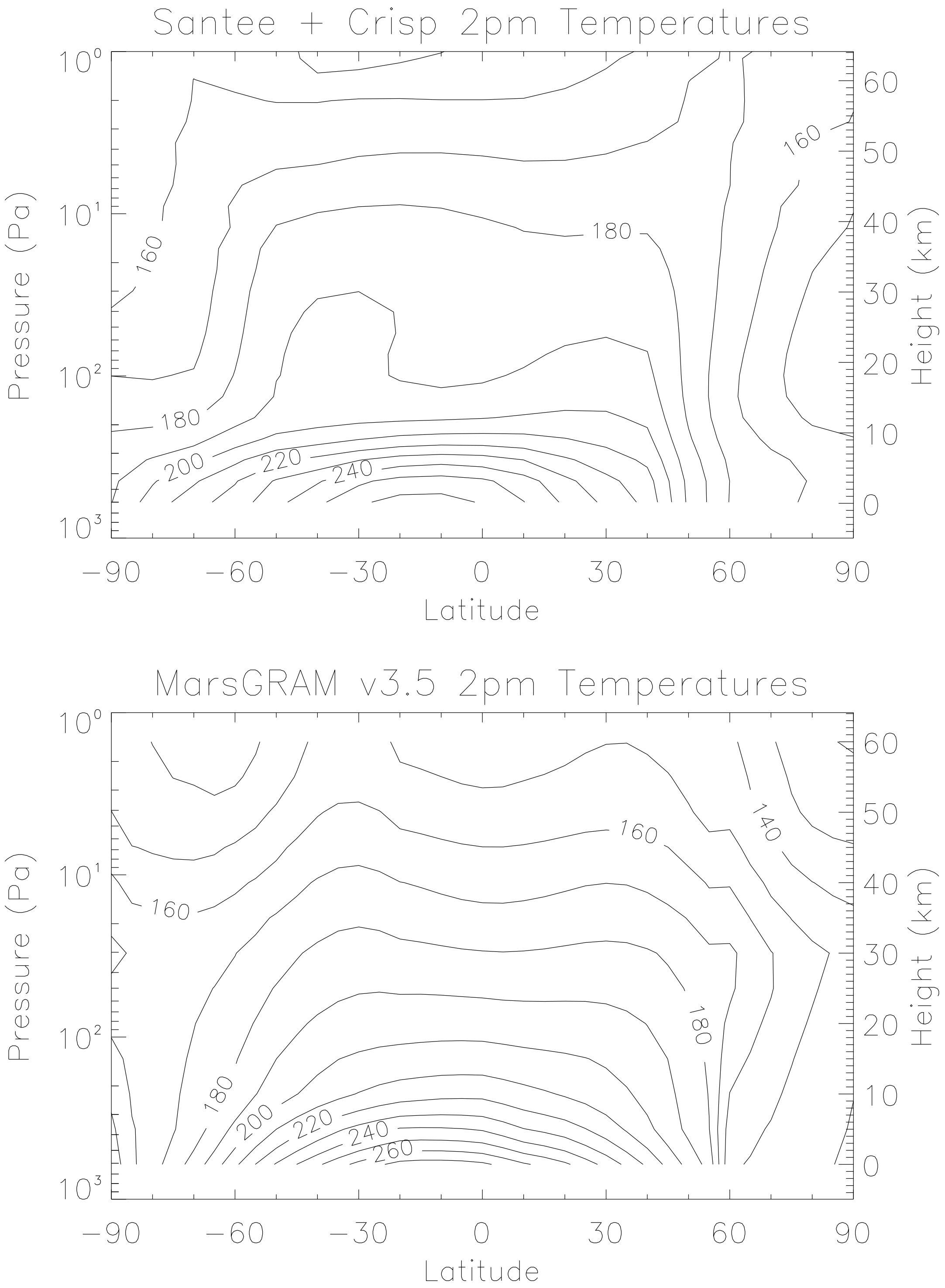

Figure 17: 2 pm temperatures for $L_s = 343°$ to $L_s = 348°$ derived by Santee and Crisp (1993) from the Mariner 9 IRIS instrument (upper figure), and the MarsGRAM 2pm temperatures for this season (lower figure).

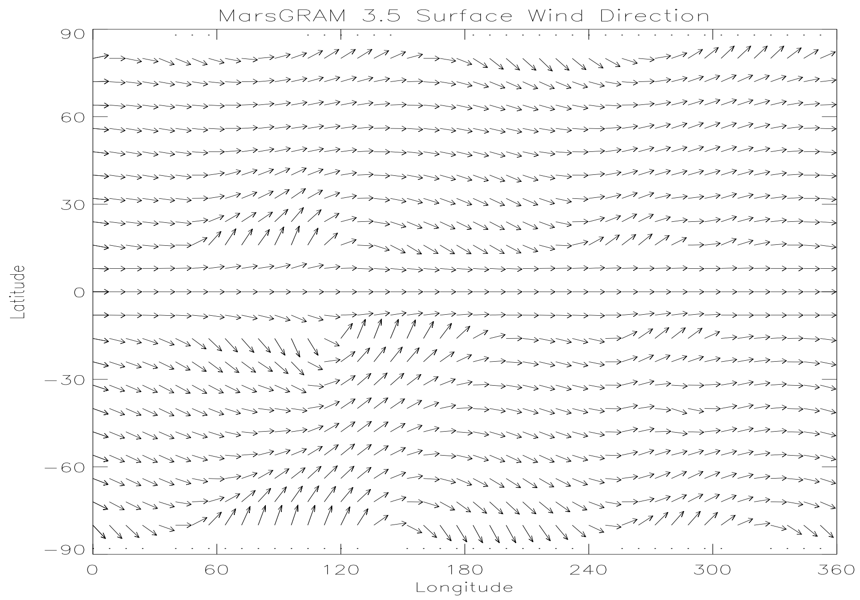

Figure 18: Low level wind directions taken from MarsGRAM v3.5 at $L_s = 270°$.

3.3 Wind

Figure 18 shows low level wind directions from MarsGRAM which should be compare with the wind streak data (fig. 8) and the MCD low level wind directions (fig. 9). MarsGRAM uses thermal wind balance to derive winds and consequently there is virtually no cross-equatorial flow (thermal wind balance is geostrophic and is therefore invalid at the equator). The MarsGRAM wind directions, therefore do not compare very well the observations. In contrast the MCD compares well as the model has considered the full dynamical wind balance when calculating the winds.

4 Summary

This document is a first comparison of the Mars Climate Database (MCD) - version 1.0 with various observational data and with the most commonly used engineering model of Mars - MarsGRAM. The MCD is broadly consistent with all the available observational data and with MarsGRAM. In addition, the strength of the MCD is that it provides a physically consistent view of the environmental conditions on Mars for the seasons and dust loadings that are not covered by the observations. Hence the MCD may be thought of as the best current estimate of the environmental conditions on Mars.

5 References

Clancy, R.T., Grossman, A.W., Wolff, M.J., James, P.B., Rudy, D.J, Billawala, Y.N., Sandor, B.J., Lee, S.W. and Muhleman, D.O. (1996) "Water vapor saturation at low altitudes around Mars aphelion: A key to Mars Climate?" *Icarus* **122,** 32–62.

Collins, M. and Lewis, S.R. (1997a) "Mars Climate Database v1.0: User Manual," *European Space Agency Report.*

Collins, M. and Lewis, S.R. (1997b) "Mars Climate Database v1.0: Detailed Design Document," *European Space Agency Report.*

Collins, M., Lewis, S.R., Read, P.L., Thomas, N.P.J., Talagrand, O., Forget, F., Fournier, R., Hourdin, F. and Huot, J.-P. (1996) "A climate database for the martian atmosphere," in *Environment Modelling for Space-based Applications,* European Space Agency **SP–392,** 323–327.

Hourdin , F., Le Van, P., Forget, F. and Talagrand, O. (1993) "Meteorological variability and the annual surface pressure cycle on Mars," *J. Atmos. Sci.* **50,** 3625–3640.

Hourdin, F., Forget, F., Fournier, R., Talagrand, O., Read, P.L., Collins, M., Lewis, S.R., Thomas, N.P.J. and Huot, J.-P. (1996) "Numerical modelling of the general circulation of the martian atmosphere," in *Environment Modelling for Space-based Applications,* European Space Agency **SP–392,** 315–320.

Justus, C.G. (1990) "A Mars Global Reference Atmosphere Model (Mars-GRAM) for mission planning and analysis," *AIAA Paper No. 90-0004,* 28th Aerospace Sciences Meeting.

Justus, C.G., Alyea, F.N., Cunnold, D.M., Jeffries, W.R. III, and Johnson, D.L. (1995) "The NASA/MSFC Global Reference Atmosphere Model - 1995 Version (GRAM-95)," *NASA Technical Memorandum.*

Leovy, C.B. (1982) "Martian meteorological variability," *Adv. Space Res.* **2,** 19–44.

Magalhaes, J.A. (1987) "The Martian Hadley circulation: Comparison of "viscous" model predictions to observations," *Icarus* **70,** 442–468.

Read, P.L., Collins, M., Lewis, S.R., Taylor, F.W., Talagrand, O., Forget, F. and Hourdin, F. (1996) "The Martian Environment," *European Space Agency Report.*

Read, P.L., Collins, M., Forget, F., Fournier, R., Hourdin, F., Lewis, S.R., Talagrand, O., Taylor, F.W. and Thomas, N.P.J. (1997) "A GCM climate database for Mars: For mission plannning and for scientific studies," *Advances in Space Research,* in press.

Zurek, R.W., Barnes, J.R., Haberle, R.M., Pollack, J.B., Tillman, J.E. and Leovy, C.B. (1992) "Dynamics of the atmosphere of Mars," in *Mars,* University of Arizona Press, Tucson, 835–933.